Branco, J.M., Verbist, M., Descamps, T. (2018, accepted manuscript). Design of three Step Joint Typologies: Review of European standardized approaches. *Engineering Structures*. (doi.org/10.1016/j.engstruct.2018.06.073)

The final publication is available at www.sciencedirect.com:
https://www.sciencedirect.com/science/article/pii/S014102961733729X

Design of three Step Joint Typologies: Review of European standardized approaches

Jorge M. Branco [a], Maxime Verbist [a] *, Thierry Descamps [b]

[a] *ISISE, Department of Civil Engineering, University of Minho, Portugal*

[b] URBAINE, *Department of Architectural Engineering, University of Mons, Belgium*

* *Corresponding author:*
ISISE, Department of Civil Engineering, University of Minho,
Campus de Azurém, 4800-058, Guimarães, *Portugal*
e-mail: verbist.maxime@hotmail.com

e-mail addresses: Jorge M. Branco - jbranco@civil.uminho.pt
Maxime Verbist - verbist.maxime@hotmail.com
Thierry Descamps - Thierry.DESCAMPS@umons.ac.be

Abstract

When assessing timber roof structures on-site for any restoration project, engineers can be faced with elements that, over time, were poorly preserved, especially damaged joints in contact with moist masonry walls. Before dealing with any intervention technique, the mechanical behaviour of such carpentry connections must be properly understood. Therefore, it has to be determined how the joints fail, which parameters (i.e. geometrical configurations and mechanical properties of the joint) influence the appearance conditions of failure modes, and the way how the internal forces are distributed within the connection. Therefore, the present paper aims at overviewing three different typologies of Step Joints (SJ) which can often be encountered within traditional timber carpentries between the rafter and the tie beam: the Single Step Joint, the Double Step Joint, and the Single Step Joint with Tenon-Mortise. Regarding each SJ typology, some design rules and geometrical recommendations can be gathered from European Standards and from authors of works on the subject, but no design equation is conventionally defined. Hence, new design models have been determined through the Analytical Campaign for the investigated Step Joints according to their geometrical parameters and to both failure modes: the shear crack in the tie beam and the crushing at the front-notch surface. In order to check the reliability of new design models and the emergence conditions of both failure modes, future experiments and numerical analysis on the three SJ typologies are going to be performed.

Keywords

Timber; Traditional carpentry connections; Step Joints; Design; Standards

Highlights

- Review of European standardized approaches;
- Geometrical and design recommendations for three Step Joint typologies;
- Mechanical behaviour of Step Joints under monotonic compression in the rafter;
- Design equations of Step Joints against shear crack and crushing;
- Reliability of design models still under discussion.

1. Introduction

In the field of Built Heritage Restoration, engineers have to work with existing timber carpentries made of poorly preserved elements and connections. Being located at the foot of timber trusses, Step Joints (SJ) are common connections used by carpenters to link the rafter to the tie beam as shown in Figure 1. Within the former and contemporary timber carpentries, three SJ typologies can often be encountered [1, 2]: the Single Step Joint, the Double Step Joint, and the Single Step Joint with Tenon-Mortise. Because they can constantly be in contact with moist masonry walls functioning as a support of the roof structure, these carpentry connections over time may be subjected to biological degradation (i.e. insect attacks, fungi decay,...), which can lead to the collapse of the whole timber truss.

Therefore, the health assessment of Step Joints on-site is a major issue for engineers involved in any restoration project dealing with existing roof structures. Before thinking about any intervention technique, the mechanical behaviour of Step Joints must be properly understood [1]. In other words, it has to be determined how the three SJ typologies fail, which parameters (i.e. geometrical configurations and mechanical properties of the joint) significantly influence the appearance conditions of the failure modes, and how the internal forces are distributed inside the connection.

Although the mechanical behaviour of existing structures is badly estimated during their on-site assessment, over time the knowledge about traditional timber carpentry connections has grown. Indeed, some geometrical and design recommendations can be obtained from European Standards (e.g. [3, 4, 5]) and from authors of other works (e.g. [2, 6, 7, 8, 9, 10, 11, 12]). However, no conventional and reliable SJ design model exists in the technical literature. Furthermore, these analytical recommendations need to be checked, optimized (if necessary) and formalized through the definition of new design models in the current Standards with respect to the appearance conditions of failure modes inside the investigated Step Joints.

In the last three decades, available scientific reports (e.g. [13, 14, 15, 16]), recent research (e.g. [17, 18, 19, 20, 21, 22, 24, 25]) and state-of-the arts (e.g. [6, 7, 12, 23, 26]) have focused on determining the mechanical behaviour of the three SJ typologies through analytical, numerical and experimental assessments. When considering only the axial force in the rafter (N_{rafter}) due to the weight of roof coverings or other permanent loads, two main failure modes illustrated in Figure 2 may occur inside the three SJ typologies: the crushing at the front-notch surface, and the shear crack in the tie beam [24]. While the former leads to high local deformation within the roof structure, the latter features a brittle failure mode that entails the collapse of the whole timber truss. Therefore, it is urgent to prevent the emergence of both failure modes, especially the shear crack, when designing and assessing on-site Step Joints. So far, the reliability of such design models for the Single Step Joint have been discussed and checked by comparing the analytical with the experimental results [24]. Besides, the design models related to the Double Step Joint have been defined in respect with both failure modes [25] whereas the design of the Single Step Joint with Tenon-Mortise has not yet been tackled.

2. Research method and assumptions

In order to fill the existing gaps in the current literature, the proposed research method consists of carrying out the Analytical Campaign on the design of three Step Joints (SJ) typologies: the Single Step Joint (SSJ), the Double Step Joint (DSJ), and the Single Step Joint with Tenon-Mortise (SSJ-TM). In the first step, the Analytical Campaign consists of gathering all the geometrical and design recommendations related to the three SJ typologies from European Standards [3, 4, 5], authors of works [2, 6, 7, 8, 9, 10, 11, 12] and recent research [23, 24, 25]. In the second step, the SJ geometrical parameters and new design models will be defined in respect with both investigated failure modes: the shear crack in the tie beam,

and the crushing at the front-notch surface. Before going ahead, several research assumptions as shown below must be firstly be established:

- As a first research assumption, only the axial force in the rafter will be considered when designing Step Joints against both failure modes [24, 25]. In other words, dynamic and out-off-plane loadings due to wind loads or earthquakes are out-of-scope. Meanwhile, this research hypothesis is highly suitable for the former carpentries without structural disorders in which timber elements are only subject to axial forces of compression or tension. Conversely, the presence of structural disorders (e.g. roof sagging, weakness or failure in support points of the structure...) and/or the current design of contemporary timber trusses may introduce significant in-plane lateral loadings in the rafter which has then to bear axial compression, bending moment and shear stresses;
- Because the rafter skew angle β highly conditions the emergence of failure modes, the three SJ typologies investigated must be characterized by a low or moderate rafter skew angle ($\beta \leq 50°$) [9]. If this research assumption is not met, another failure mode may appear such as a crushing at the bottom-notch surface within Step Joints due to the high vertical component loadings transferred from the rafter;
- In case of SJ bad design, other failure modes illustrated in Figure 2 may occur: the crushing perpendicular to the grain at the bottom of the tie beam along the support, the tensile crack and the rolling shear failure at the SJ heel in the tie beam cross-section. While the crushing can be avoided by increasing properly the support length l_{supp} at the foot of timber truss, the tensile and rolling shear failures can be prevented by checking the geometrical recommendations on the heel depth [6] for each SJ typology. Otherwise, further design equations (not detailed in the present paper) should be established to prevent these extra failure modes;
- Because the mathematical equations from the SJ design models have to be as simple as possible, friction forces can be neglected because they are usually weak at

unreinforced contact surfaces of such traditional carpentry connections. On the other hand, friction forces should be considered when designing any SJ strengthening at the contact surfaces;

- Furthermore, when designing Step Joints the eccentricity between the joint node (i.e. intersection between the rafter and tie beam axes) and the support area of timber trusses (d_{supp}) shown in Figure 2 must be controlled. If the condition $d_{supp} \leq h_{tb}$ checks with the tie beam height (h_{tb}), the eccentricity effects can be neglected [9]. Otherwise, the internal resolution forces will not be balanced between the joint node and the support area, which entails the appearance of the bending moment with added compressive, tensile and shear stress at the SJ heel in the tie beam cross-section;
- And, last but not least, Step Joints must be sound, exempt of any damage (i.e. gaps at contact surfaces, shrinkage splitting, insect attacks, fungi decay,...). However, this research assumption cannot be easily met because the existing timber roof structures are often found as having poorly preserved elements and joints. Hence, the SJ design models introduced in the present paper must be very carefully used when assessing and designing the existing Step Joints in the scope of a restoration project.

In order to prevent the emergence of failure modes, the SJ design consists of checking the general equation (1) where both parameters N_{rafter} and $N_{rafter,Rd}$ are respectively the axial force in the rafter and the design rafter load-bearing capacity of the connection. Conform with NBN EN 1995-1-1 (2.14) [3], the equation (2) defines the design and characteristic values of a wood strength property (respectively noted X_d and X_k), by taking into account the modification factor for duration of load and moisture content (k_{mod}) and the partial coefficient of wood material (γ_M).

$$N_{rafter} \leq N_{rafter,Rd} \quad (1)$$

$$X_d = X_k \cdot \frac{k_{mod}}{\gamma_M} \quad (2)$$

3. Analytical Campaign

The present Analytical Campaign aims at overviewing three Step Joints (SJ) commonly encountered within existing timber carpentries: the Single Step Joint, the Double Step Joint, and the Single Step Joint with Tenon-Mortise. According to European Standards and to authors of other works, the geometrical parameters must be determined for each SJ typology while new design models have to be defined in according with both failure modes.

3.1 Single Step Joint (SSJ) Design

When predicting the emergence of both failure modes and the strength of Single Step Joint, the geometrical parameters of the connection and wood mechanical properties must be defined. Afterwards, design equations can be proposed for the Single Step Joint against shear crack and crushing.

3.1.1 Geometrical parameters

The Single Step Joint (SSJ) is the most common connection used to link the rafter with the tie beam due to its simple geometrical configuration [1]. As illustrated in Figure 3, the SSJ geometrical configuration is characterized by a single heel, including two contact surfaces, between the rafter and the tie beam. The first contact area, called “front-notch surface’’, is located in the front of the joint whereas the last one, called “bottom-notch surface”, is situated at the bottom of the same connection. The front-notch surface is inclined under an angle α to the normal of the grain in the tie beam whereas the parameter γ is the inclination angle of the bottom-notch surface in respect with the grain.

From past to contemporary timber trusses, one may identify three SSJ families [2] shown in Figure 3, based on the inclination angle α of the front-notch surface: the Geometrical Configuration Ideal Design (GCID) with $\alpha = \beta/2$, the Geometrical Configuration Perpendicular to the Tie Beam (GCPTB) with $\alpha = 0°$, and the Geometrical Configuration Perpendicular to the Rafter (GCPR) with $\alpha = \beta$. Being the most efficient joint, the GCID is

nevertheless the most recent one because its geometry requires an accurate cutting of timber, by using new technologies (e.g. Computer Numerical Control (CNC)).

The Single Step Joint is also featured by the heel depth t_v, the shear length l_v, and the rafter skew angle β. From the work of Siem and Jorissen [6], some recommendations about the SSJ geometrical parameters can be proposed from several European Standards and National Annexes [4, 5, 27, 28, 29, 30, 31, 32, 33, 34], as given in Table 1. If the prescriptions regarding the maximum heel depth t_v cannot be met, further design equations (not overviewed in the present paper) must be taken into account in order to prevent the tensile crack and/or rolling shear failure when designing the tie beam cross-section.

3.1.2 Calculation of the characteristic compressive strength

Because the inclination angle α of the front-notch surface may vary at the rafter and tie beam sides, the design compressive strength of $f_{c,\alpha,d}$ under an angle α to the grain can be estimated by using empirical equations such as Hankinson's or Norris's Criteria [6, 7, 23]. As per NBN EN 1995-1-1 (6.16) [3], Hankinson's Criterion (3) is based on the combination of the design compressive strengths parallel $f_{c,0,d}$ and perpendicular $f_{c,90,d}$ to the grain. Another version of Hankinson's Criterion (4) can be found in the Swiss Standard SIA 265 [5] by reducing the mechanical properties by the factor of 0.8. As the use conditions of compressive loading factor $k_{c,90}$ is not defined by the NBN EN 1995-1-1 [3] when it comes to designing traditional carpentry connections, it can then be dismissed ($k_{c,90} = 1$) for the simplification of design calculations [6, 7].

In addition to these compressive strengths, Norris's Criterion (5)-(6)-(7) from the German Standard DIN 1052 (51)-(52) [4] also includes the design shear strength $f_{v,d}$ parallel to the grain, and the compressive loading factor $k_{c,\alpha}$ (7) under an inclination angle α to the grain. In accordance with the German National Annex of Eurocode 5 [28] and with DIN 1052 (284) [4], from the literature [6, 7, 23], the modified Norris's Criterion can be defined by (8) where both $f_{v,d}$ and $f_{c,90,d}$ rise by the factor of 2.

$$\sigma_{c,\alpha,d} \leq f_{c,\alpha,d} = \frac{f_{c,0,d}}{\frac{f_{c,0,d}}{k_{c.90} \cdot f_{c,90,d}} sin^2(\alpha) + cos^2(\alpha)} \quad (3)$$

$$\sigma_{c,\alpha,d} \leq f_{c,a,d} = \frac{0.8 \,.\, f_{c,0,d} \cdot f_{c,90,d}}{0.8 \,.\, f_{c,0,d} \,.\, sin^2(\alpha) + f_{c,90,d} \,.\, cos^2(\alpha)} \quad (4)$$

$$\sigma_{c,\alpha,d} \leq k_{c,\alpha} \,.\, f_{c,a,d} \quad (5)$$

$$f_{c,a,d} = \frac{f_{c,0,d}}{\sqrt{\left(\frac{f_{c,0,d}}{f_{c,90,d}} \sin^2(\alpha)\right)^2 + \left(\frac{f_{c,0,d}}{1.5 \cdot f_{v,d}} \sin(\alpha) \,.\, \cos(\alpha)\right)^2 + cos^4(\alpha)}} \quad (6)$$

$$k_{c,\alpha} = 1 + \sin\alpha \,.(k_{c,90} - 1) \quad (7)$$

$$\sigma_{c,\alpha,d} \leq f_{c,a,d} = \frac{f_{c,0,d}}{\sqrt{\left(\frac{f_{c,0,d}}{2 \cdot f_{c,90,d}} \sin^2(\alpha)\right)^2 + \left(\frac{f_{c,0,d}}{2 \cdot f_{v,d}} \sin(\alpha) \,.\, \cos(\alpha)\right)^2 + cos^4(\alpha)}} \quad (8)$$

where:

$f_{c,0,d}$ is the design compressive strength parallel to the grain;

$f_{c,\alpha,d}$ is the design compressive strength inclined under an angle α to the grain;

$f_{c,90,d}$ is the design compressive strength perpendicular to the grain;

$f_{v,d}$ is the design shear strength;

$k_{c,\alpha}$ is the factor of the compressive stress spreading under an angle α to the grain inside timber;

$k_{c,90}$ is the factor of the compressive stress spreading perpendicular to the grain inside timber;

α is the inclination angle of the compressive loading with respect to the grain;

$\sigma_{c,\alpha,d}$ is the design compressive stress inclined under an angle α to the grain.

3.1.3 SSJ Design model against the shear crack

As shown in Figure 4, the design rafter load-bearing capacity, noted $N_{rafter,Rd}$, must be checked by the equations (1)-(9)(10)-(11) in order to prevent the emergence of shear crack in the tie beam [6, 7, 8, 9, 23, 24]. Based on the maximal limitation of the shear length ($l_{v,max} = 8.t_v$) indicated by DIN 1052 [4] in Table 1, the effective shear length $l_{v,eff}$ takes into account the non-uniform shear stress distribution τ_{Ed} along the grain at the heel depth in the tie beam. From the equation (10), the effective shear length encompasses the significant shear stress distribution whose the concentration peak is always located at the SSJ heel. Furthermore, the reducer coefficient noted $k_{v,red}$ takes into account the presence of non-uniform shear stress distribution at the heel depth along the grain in the tie beam,

which entails the decrease of shear capacity of the Single Step Joint. As per the Dutch National Annex of Eurocode 5 [30], from the work of Siem and Jorissen [6], the value of the reducer coefficient $k_{v,red} = 0.8$ can then be applied to the design shear strength of timber parallel to the grain in the tie beam, noted $f_{v,d}$. Hence, the equation (11) have to be checked by comparing the reduced design shear strength $f_{v,red,d}$ with the design average of shear stress $\tau_{m,d}$ uniformly distributed over the effective shear length $l_{v,eff}$ as illustrated in Figure 4.

$$N_{rafter,Rd} = f_{v,red,d} \cdot \frac{b \cdot k_{cr} \cdot l_{v,eff}}{\cos \beta} \quad (9)$$

$$l_{v,eff} = min(l_v, 8.t_v) \quad (10)$$

$$\tau_{m,d} \leq f_{v,red,d} = k_{v,red} \cdot f_{v,d} \quad (11)$$

where:

$N_{rafter,Rd}$	is the design rafter load-bearing capacity;
$f_{v,d}$	is the design shear strength;
$f_{v,red,d}$	is the reduced design shear strength;
k_{cr}	is the crack factor for the shear strength;
$k_{v,red}$	is the reducer coefficient of the shear strength;
β	is the rafter skew angle;
b	is the tie beam width;
l_v	is the shear length;
$l_{v,eff}$	is the effective shear length of the tie beam;
t_v	is the heel depth of the tie beam;
$\tau_{m,d}$	is the design average of shear stress.

In accordance with Amendment 1 of Eurocode 5 (6.13a) [35], the crack factor k_{cr}=0.67 (solid timber) can be imposed to reduce the tie beam width *b*, by considering the impact of longitudinal cracks on the shear strength along the grain for the timber element subject to bending or to wetting-drying cycles. If the condition $d_{supp} \leq h_{tb}$ is checked (Figure 2), the eccentricity effects including extra bending moment and cracks appearance in the tie beam can be neglected [9]. In that case, the crack factor can be disregarded ($k_{cr} = 1$) for the tie beam featuring no drying crack.

3.1.4 SSJ Design model against the crushing

As illustrated in Figure 5, the design rafter load-bearing capacity, noted $N_{rafter,Rd}$, must be checked at the rafter side by the equations (1)-(12)-(13), and at the tie beam side by (1)-(14)-(15), in order to avoid the crushing at the front-notch surface for the GCID ($\alpha = \beta/2$) [6, 7, 8, 9, 23, 24] and for the other SSJ geometrical configurations characterized by $\alpha \in]0, \beta[$. Concerning the GCPTB featured by an inclination angle of the front-notch surface $\alpha = 0°$, the crushing always occurs at the rafter side as the related design compressive strength ($f_{c,\alpha=\beta,d}$) is lower than that at the tie beam side ($f_{c,0,d}$). Hence, the design rafter load-bearing capacity from the GCPTB, noted $N_{rafter,Rd}$, must be checked at the rafter side by the equations (1)-(12)-(13) with $\alpha = 0°$ [24]. In contrast to the GCPTB, the crushing always appears at the tie beam side for the GCPR as the front-notch surface from this SSJ configuration is inclined under an angle $\alpha = \beta$. Therefore, the design rafter load-bearing capacity from the GCPR, noted$N_{rafter,Rd}$, must be checked at the tie beam side by the equations (1)-(15)-(16) [24]. The definition of effective compressive lengths $t_{ef,rafter}$ and $t_{ef,tb}$ from Bocquet [8] is based on the interpretation of EN 1995-1-1 [3] and DIN 1052 [4] for the spreading of compressive stress perpendicular to the grain over 30 mm depth inside timber.

$$N_{rafter,Rd} = f_{c,\beta-\alpha,d} \cdot \frac{b.\, t_{ef,rafter} \,.\, sin(90+\alpha-\gamma)}{sin(90-\beta+\gamma)} \quad (12)$$

$$t_{ef,rafter} = \frac{t_v}{\cos(\alpha)} + 30\ sin(\beta-\alpha) + 30\sin(\alpha-\gamma) \quad (13)$$

$$N_{rafter,Rd} = f_{c,\alpha,d} \cdot \frac{b.\, t_{ef,tb} \,.\, sin(90+\alpha-\gamma)}{sin(90-\beta+\gamma)} \quad (14)$$

$$t_{ef,tb} = \frac{t_v}{cos(\alpha)} + 30\ tan(\alpha) + 30 \quad (15)$$

$$N_{rafter,Rd} = f_{c,\alpha,d} \,.\, b \,.\, t_{ef,tb} \quad (16)$$

where:

$N_{rafter,Rd}$ is the design rafter load-bearing capacity;

$f_{c,\alpha,d}$ is the design compressive strength inclined under an angle α to the grain at the tie beam side;

$f_{c,\beta-\alpha,d}$ is the design compressive strength inclined under an angle $\beta - \alpha$ to the grain at the rafter side;

α is the inclination angle of the front-notch surface with respect to the normal of the grain in the tie beam;

β is the rafter skew angle;

γ is the inclination angle of the bottom-notch surface with respect to the grain in the tie beam;

b is the tie beam width;

$t_{ef,rafter}$ is the effective compressive length of the front-notch surface at the rafter side;

$t_{ef,tb}$ is the effective compressive length of the front-notch surface at the tie beam side;

t_v is the heel depth of the tie beam.

3.2 Double Step Joint (DSJ) Design

Because the emergence conditions of shear crack and crushing have to be established with respect to the Front and Rear Heels, the geometrical parameters of Double Step Joint must be overviewed. Last but not least, design equations can be proposed against shear crack and crushing in both heels of the connection.

3.2.1 Geometrical parameters

Although the Single Step Joint (SSJ) is the most common joint used to link the rafter with the tie beam, the Double Step Joint (DSJ) is sometimes found within traditional timber carpentries, as illustrated in Figure 6. When, for example, the limitation of the SSJ shear length l_v is too small due to geometrical restrictions, the Double Step Joint can be used instead of the Single Step Joint in order to better prevent the shear crack, providing higher shear capacity in the tie beam. Because the Double Step Joint is featured by both heels, the shear length in the tie beam is then higher than that of the Single Step Joint. Nevertheless, the DSJ design requires an accurate cutting of timber by using new available technologies (e.g. CNC).

As shown in Figure 7, the “Front Heel” is located in the front of the Double Step Joint while the “Rear Heel” is situated in the rear of the same connection. Similar to the Single Step Joint, each DSJ heel includes two contact surfaces between the rafter and the tie beam: the front-notch surface, which is located in the front of the heel, and the bottom-notch surface,

situated at the bottom. Whereas the inclination angles of the front-notch and bottom-notch surfaces (i.e. α_1 and γ_1, respectively) in the Front Heel are identical to the three SSJ families (i.e. GCID, GCPTB and GCPR) [2], those in the Rear Heel are related to the GCPR and $\alpha_2 = \gamma_2 = \beta$. The shear length at the Front Heel depth $t_{v,1}$, noted $l_{v,1}$, is the distance between the top of the Front Heel and the tie beam edge along the grain while the shear length at the Rear Heel depth $t_{v,2}$, noted $l_{v,2}$, is the distance between the top of both heels along the tie beam grain. From the work of Siem and Jorissen [6], some recommendations about the DSJ geometrical parameters can be proposed based on several European Standards and National Annexes [4, 5, 29, 30, 34], as given in Table 2.

Furthermore, it is crucial to meet the geometrical requirement $\Delta t_v \geq 10\ mm$, where Δt_v is the difference between the Front and Rear Heels depths, in order to ensure the correct development of the shear crack in the tie beam. From German and Swiss Standards [4, 5], the maximal values of $t_{v,1}$ and $t_{v,2}$ as well as the minimal value of Δt_v cannot however be checked together when the tie beam height is small ($h_{tb} < 120\ mm$). In accordance with the Italian Standard [29], no limitation of the Rear Heel depth $t_{v,2}$ with respect to the tie beam height h_{tb} is explicitly defined for the Double Step Joint (Table 2), while the geometrical condition $t_v \leq h_{tb}/4$ has to be met for the Single Step Joint featuring by low and moderate rafter skew angles $\beta \leq 50°$ (Table 1). Because it aims at preventing high tensile stress and rolling shear stress in the reduced tie beam cross-section, the geometrical requirement $t_{v,2} \leq h_{tb}/4$ should also be applied for the Italian Standard [29] in the Table 2, in order to limit the maximal value of the Rear Heel depth.

3.2.2 DSJ design model against the shear crack

As illustrated in Figure 8, the design rafter load-bearing capacity, noted $N_{rafter,Rd,i}$, must be checked by the equations (1)-(17)-(18)-(19), similar to (9)-(10)-(11) from the SSJ design, in order to prevent the appearance of shear crack in the tie beam for each DSJ heel [6-8, 25].

$$N_{rafter,Rd,i} = f_{v,red,d,i} \cdot \frac{b \cdot k_{cr} \cdot l_{v,eff,i}}{\cos \beta} \quad (17)$$

$$l_{v,eff,i} = \min(l_{v,i}, 8.\, t_{v,i}) \quad (18)$$

$$\tau_{m,d,i} \leq f_{v,red,d,i} = k_{v,red,i} \cdot f_{v,d} \quad (19)$$

where:

i	is the type of DSJ heel (i.e. i=1 for the Front Heel, i=2 for the Rear Heel);
$N_{rafter,Rd,i}$	is the design rafter load-bearing capacity according to the type of DSJ heel;
$f_{v,d}$	is the design shear strength;
$f_{v,red,d,i}$	is the reduced design shear strength according to the type of DSJ heel;
k_{cr}	is the crack factor for the shear strength;
$k_{v,red,i}$	is the reducer coefficient of the shear strength related to the type of DSJ heel;
β	is the rafter skew angle;
b	is the tie beam width;
$l_{v,i}$	is the shear length with respect to the type of DSJ heel;
$l_{v,eff,i}$	is the effective shear length of the tie beam with respect to the type of DSJ heel;
$t_{v,i}$	is the heel depth of the tie beam with respect to the type of DSJ heel;
$\tau_{m,d,i}$	is the design average of shear stress according to the type of DSJ heel.

Based on the maximal limitation of the shear length ($l_{v,max,i} = 8.\, t_{v,i}$) imposed by DIN 1052 [4] indicated in Table 2, the effective shear lengths $l_{v,eff,i}$ take into account the non-uniform shear stress distributions $\tau_{Ed,i}$ in the tie beam for both DSJ heels. In respect with the equation (18), the effective shear lengths then encompass both significant shear stress distributions for which the related concentration peaks are always located at the Front and Rear Heels as shown in Figure 8. The reducer coefficients noted $k_{v,red,i}$ consider the presence of the non-uniform shear stress distribution at both DSJ heel depths along the grain in the tie beam. The condition $k_{v,red,i} = 0.8$ could then be applied to the design shear strength $f_{v,red,i}$ (19) in the Front and Rear Heels in order to compare the reduced design shear strengths $f_{v,red,d,i}$ with the design average shear stresses $\tau_{m,d,i}$ uniformly distributed over the related effective shear lengths $l_{v,eff,i}$, as illustrated in Figure 8. The recommended values of the crack factor k_{cr} from the SSJ design against the shear crack can also be applied for the Double Step Joint.

According to Bocquet [8], a 1-2 mm gap is preconized at the front-notch surface in the Front Heel for the DSJ design against the shear crack. When the front-notch surfaces from the

rafter and tie beam sides finally come into contact in the Front Heel due to high crushing in the Rear Heel, the internal forces distribution becomes ideal because it is balanced between both DSJ heels. As a result, the design rafter load-bearing capacities $N_{rafter,Rd,i}$, firstly governed by crushing at the front-notch surface (i.e. plastic failure), can reach their maximal values in the Rear and then the Front Heels. However, the shear crack illustrated in Figure 8 may emerge in the tie beam, at the Front and Rear Heels depths (i.e. $t_{v,1}$ and $t_{v,2}$) over their respective shear lengths (i.e. $l_{v,1}$ and $l_{v,2}$), as the final failure mode after high crushing in the Double Step Joint [24, 25]. In order to prevent this brittle failure mode, the maximal design rafter load-bearing capacity, noted $N_{rafter,Rd,max}$, must be checked by (1)-(20) [25] as well as the sum of the design rafter load-bearing capacities related to both DSJ heels given by equation (17).

$$N_{rafter,Rd,max} = N_{rafter,Rd,1} + N_{rafter,Rd,2} \quad (20)$$

If the Double Step Joint does not feature any gap at its contact surfaces, the internal forces distribution is not ideal because most of the axial force in the rafter (N_{rafter}) will directly be transferred into the Front Heel characterized by lower compressive and shear capacities. In that case, the design rafter load-bearing capacity from the Rear Heel ($N_{rafter,Rd,2}$) does not reach its maximal value and the emergence of shear crack will only occur at the Front Heel depth $t_{v,1}$ along the grain in the tie beam. Hence, the total design rafter load-bearing capacity (21) [25], noted $N_{rafter,Rd,tot}$, is always between the design rafter load-bearing capacity related to the Front Heel ($N_{rafter,Rd,1}$) and the maximal design rafter load-bearing capacity ($N_{rafter,Rd,max}$), from equations (17) and (20).

$$N_{rafter,Rd,1} \leq N_{rafter,Rd,tot} \leq N_{rafter,Rd,max} \quad (21)$$

3.2.3 DSJ design model against the crushing

As illustrated in Figure 9, the design rafter load-bearing capacity against the crushing at the front-notch surface in the Front Heel, noted $N_{rafter,Rd,1}$, must be checked by the equations (12)-(13)-(14)-(15)-(16) in respect with the three SSJ families. The design rafter load-bearing

capacity against the crushing at the front-notch surface in the Rear Heel, noted $N_{rafter,Rd,2}$, must be checked by the GCPR design equation (16), based on the effective length $t_{ef,tb,2}$ (22) [25] at the tie beam side as shown in Figure 10.

$$t_{ef,tb,2} = \frac{t_{v,2}}{cos(\beta)} + 30\ tan(\beta - \gamma_1) + 30 \quad (22)$$

Conform with Bocquet [8], 1-2 mm gap should ideally be present at the front-notch surface in the Front Heel for the DSJ design against the crushing. If the geometrical requirement is met, the internal forces resolution becomes ideal so that the design rafter load-bearing capacities related to the Front and Rear Heels (i.e. $N_{rafter,Rd,1}$ and $N_{rafter,Rd,2}$, respectively) can reach their maximal values. In order to prevent the crushing at the front-notch surface, the maximal design rafter load-bearing capacity, noted $N_{rafter,Rd,max}$, must be checked by (1)-(20) such as the sum of design rafter load-bearing capacities related to the Front and Rear Heels.

If the Double Step Joint does not feature any gap at its contact surfaces, the internal forces resolution is then not ideal. Because the Front Heel depth $t_{v,1}$ is inferior to the Rear Heel depth $t_{v,2}$, the design rafter load-bearing capacity from the Front Heel will probably reach its maximal value before that from the Rear Heel does. Being determined by the equation (21), the total design rafter load-bearing capacity, noted $N_{rafter,Rd,tot}$, is always between the design rafter load-bearing capacity related to the Front Heel ($N_{rafter,Rd,1}$) and the maximal design rafter load-bearing capacity ($N_{rafter,Rd,max}$) against the crushing at the front-notch surfaces.

Meanwhile, the compressive capacities related to both DSJ heels may progressively develop with high crushing in the connection. Being characterized by a plastic failure mode, the crushing at the front-notch surface in the Front Heel causes high deformation, leading to the grain densification [24]. As the timber locally densify at this contact area of the joint, the compressive stress and the related design rafter load-bearing capacity $N_{rafter,Rd,1}$ may slightly rise with the crushing. On the other hand, the internal forces distribution in the Double Step Joint may change due to high displacement of the Front Heel. As a result, higher

compressive stress may occur at the front-notch surface in the Rear Heel for which the design rafter load-bearing capacity $N_{rafter,Rd,2}$ is still increasing till reaching its maximal value predicted by the equations (16)-(22).

3.3 Single Step Joint with Tenon-Mortise (SSJ-TM) Design

Regarding the last step of the Analytical Campaign, the geometrical parameters of the Single Step Joint with Tenon-Mortise must be determined in order to establish the emergence conditions of both failure modes. As a result, design equations can be proposed for this typology of Step Joint against shear crack and crushing.

3.3.1 Geometrical parameters

When higher shear and compressive capacities are required to guarantee the structural safety of timber trusses against both failure modes investigated, the Single Step Joint with Tenon-Mortise (SSJ-TM) illustrated in Figure 11, can be used instead of the Single Step Joint (SSJ) in order to link the tie beam with the rafter. Because this carpentry connection is also featured by a complex geometry, accurate timber cutting ensured by skilled carpenters or new technologies use (e.g. CNC) is necessary to design the Single Step Joint with Tenon-Mortise. Nevertheless, it appears more often than the Double Step Joint (DSJ) within existing timber carpentries like for the classical Tenon-Mortise connections [10].

As shown in Figure 11, the Single Step Joint with Tenon-Mortise is characterized by a Tenon at the rafter side and by a Mortise at the tie beam side. Among the three SJ typologies overviewed in the present paper, the Single Step Joint with Tenon-Mortise features the largest amount of contact surfaces grouped into two parts. As illustrated in Figures 11 and 12, the Single Step Joint (SSJ) part includes one front-notch surface, and two bottom-notch surfaces called “shoulders”. On the other hand, the Tenon-Mortise (TM) part contains one front-notch surface, two bottom-notch surfaces, and two lateral surfaces. Note that the TM part provides significant bending moment capacity to the Step Joint which may be subject to loadings in out-off-plane directions. The inclination angle α of the front-notch surface and

the inclination angle γ of shoulders are identical from those previously stated for the Single Step Joint without Tenon-Mortise. Although several orientations of both bottom-notch surfaces in the TM part exist in the literature [2, 10, 11], one of both bottom-notch surfaces is usually parallel to the grain in the tie beam whereas the other one is the extension from the rafter edge direction as shown in Figure 12.

Furthermore, two parts must be distinguished within the SSJ-TM heel: the SSJ Heel, and the TM Heel. The former is characterized by the shoulder heel depth t_S, identical to the heel depth t_v from the Single Step Joint without Tenon-Mortise, whereas the latter is featured by the heel depth noted t_{TM}. In accordance with the geometrical requirements from the literature [2, 10, 11, 12], the TM width noted b_{TM} should ideally be equal to the shoulder width b_S (i.e. one-third of the tie beam width b) in order to balance their respective compressive capacities perpendicular to the grain in the tie beam.. Being conditioned by small TM width b_{TM}, the horizontal bottom-notch surface in the TM part then becomes the weakest component of the joint as concerns its compressive capacity perpendicular to the grain. To overcome this weakness, a 5 mm gap can be designed at the bottom-notch surface between the Tenon and the Mortise, by preventing any vertical loading transfer on that area [12]. In that case, the internal forces of the joint can only be distributed at the front-notch surface and shoulders.

When the vertical load component rises in the shoulders with higher rafter skew angles ($\beta > 50°$), the mechanical behaviour of the Single Step Joint with Tenon-Mortise governed by the compressive crushing perpendicular to the grain in the tie beam is then not optimal, compared to the Single or Double Step Joints. For low and moderate rafter skew angles ($\beta \leq 50°$), it is better to increase the TM Heel depth t_{TM} as much as possible in order to bear the significant rafter thrust inside the joint which entails the appearance of shear crack in the tie beam and/or crushing at the front-notch surface. However, the parameter t_{TM} should not exceed the half-height of the tie beam h_{tb}, in order to avoid high tensile stresses parallel to the grain and rolling shear stresses perpendicular to the grain in the reduced tie

beam cross-section. Apart from these few recommendations, no conventional rule is defined for the other SSJ-TM geometrical parameters. However, the SSJ geometrical recommendations from the Table 1 can be used for the third SJ typology when substituting the SSJ Heel depth t_v by the shoulder heel depth t_S.

3.3.2 SSJ-TM design model against the shear crack

As shown in Figure 13, the design rafter load-bearing capacity, noted $N_{rafter,Rd}$, must be checked by (1)-(23), in order to prevent the appearance of shear crack at the heel depth t_v (i.e. the TM Heel depth t_{TM}) along the grain in the tie beam. Like for the Single Step Joint with Double Tenon-Mortise [8], two subcategories of failure modes related to the shear crack must be considered when designing the Single Step Joint with Tenon-Mortise. As illustrated in Figure 14, the overall shear crack at the TM Heel depth along the grain in the tie beam can be induced either by the T-shaped shear block along the path of both shoulders, or by the tensile crack in their respective cross-sections. Therefore, the overall shear crack, the T-shaped shear block and the tensile crack must be avoided by checking the following equations (24), (25) and (26) respectively [8].

$$N_{rafter,Rd} = max\begin{Bmatrix} F_{v,tb} \\ min\{F_{v,s}\,;\, F_{t,s}\} \end{Bmatrix} \quad (23)$$

$$F_{v,tb} = f_{v,red,d} \cdot \frac{b \,.\, k_{cr} \,.\, l_{v,eff}}{\cos\beta} \quad (24)$$

$$F_{v,s} = f_{v,red,d} \cdot \frac{(2\,.(t_{TM} - t_S) + b) \,.\, k_{cr} \,.\, l_{v,eff}}{\cos\beta} \quad (25)$$

$$F_{t,s} = f_{t,0,d} \,.\, k_{dis} \,.\, k_{vol} \cdot \frac{2\, b_S \,.\, (t_{TM} - t_S)}{\cos\beta} \quad (26)$$

where:

$N_{rafter,Rd}$ is the design rafter load-bearing capacity;
$F_{v,tb}$ is the overall shear capacity at the TM heel depth in the tie beam;
$F_{v,s}$ is the shear block capacity along the path of shoulders in the tie beam;
$F_{t,s}$ is the tensile capacity in the shoulders cross-section;
$f_{v,red,d}$ is the reduced design shear strength;
$f_{t,0,d}$ is the design tensile strength parallel to the grain;
k_{cr} is the crack factor for the shear strength;
k_{dis} is the factor of the tensile stress distribution in the stressed volume;
k_{vol} is the factor of the volume subject to tensile stresses;

β is the rafter skew angle;
b is the tie beam width;
b_S is the shoulder width in the tie beam;
$l_{v,eff}$ is the effective shear length in the tie beam;
t_S is the shoulder heel depth in the tie beam;
t_{TM} is the TM heel depth in the tie beam.

The appearance of either the T-shaped shear block or the tensile crack in the shoulders of the tie beam is conditioned by the difference between the TM and SSJ Heels depths, noted Δt_v. Higher the geometrical parameter Δt_v, higher the risk of the T-shaped shear block to occur in the tie beam because the tensile capacity of the shoulders $F_{t,s}$ becomes superior to their related shear block capacity $F_{v,s}$. In that case, the design rafter load-bearing capacity $N_{rafter,Rd}$ is governed by the T-shaped shear block, which significantly enhances the shear capacity of the joint ($F_{v,s}$), compared to the overall shear capacity at the TM Heel depth in the tie beam ($F_{v,tb}$). Therefore, the emergence of T-shaped shear block must be ensured through using high values of Δt_v in order to optimize the mechanical behaviour of the Single Step Joint with Tenon-Mortise against the shear crack.

Similar to the other two SJ typologies, the non-uniform shear stress distribution τ_{Ed} appears at the TM heel depth along the grain in the tie beam as shown in Figure 13, by reducing the shear capacity of the connection. To this end, the effective shear length $l_{v,eff}$ (10) and the reducer coefficient $k_{v,red} = 0.8$ from the Single Step Joint without Tenon-Mortise can also be applied when determining the reduced design shear strength $f_{v,red,d}$ (11) in the Single Step Joint with Tenon-Mortise. Due to the presence of non-uniform tensile stress distribution parallel to the grain in the shoulders cross-section, the distribution and volume factors from Eurocode 5 [3], noted k_{dis} and k_{vol} respectively, must be taken into account when calculating the tensile capacity of shoulders $F_{t,s}$. Whereas $k_{vol} = 1$ is imposed for solid timber [3], $k_{dist} = 1$ can be suggested as its use conditions for carpentry joints are not defined in European Standards.

3.3.3 SSJ-TM design model against the crushing

As illustrated in Figure 15, the design rafter load-bearing capacity, noted $N_{rafter,Rd}$, must be checked at the rafter side by the equations (1)-(13)-(27)-(28)-(29) and at the tie beam side by (1)-(15)-(30)-(31)-(32), in order to avoid the crushing at the front-notch surface for the GCID ($\alpha = \beta/2$) and for the other SSJ-TM geometrical configurations characterized by $\alpha \in]0, \beta[$. Note that the effective lengths in the shoulders at the rafter and tie beam sides, noted $t_{S,ef,rafter}$ and $t_{S,ef,tb}$, are equivalent to the effective lengths in the rafter $t_{ef,rafter}$ (13) and in the tie beam $t_{ef,tb}$ (15) from the Single Step Joint without Tenon-Mortise. Concerning the GCPTB characterized by an inclination angle of the front-notch surface $\alpha = 0°$, the crushing always occurs at the rafter side because the related design compressive strength ($f_{c,\alpha=\beta,d}$) is lower than that at the tie beam side ($f_{c,0,d}$). Hence, the design rafter load-bearing capacity from the GCPTB, noted $N_{rafter,Rd}$, must be checked at the rafter side by the equations (1)-(13)-(27)-(28)-(29). In contrast to the GCPTB, the crushing always appears at the tie beam side for the GCPR because the related front-notch surface is inclined under an angle $\alpha = \beta$. Thereby, the design rafter load-bearing capacity from the GCPR, noted $N_{rafter,Rd}$, must be checked at the tie beam side by the equations (1)-(15)-(31)-(32)-(33).

$$N_{rafter,Rd} = f_{c,\beta-\alpha,d} \cdot \frac{A_{c,ef,rafter} \cdot sin(90+\alpha-\gamma)}{sin(90-\beta+\gamma)} \quad (27)$$

$$A_{c,ef,rafter} = b.t_{S,ef,rafter} + (b - 2b_S).t_{TM,ef,rafter} \quad (28)$$

$$t_{TM,ef,rafter} = \frac{t_{TM}-t_S}{\cos(\alpha)} + \frac{30\sin(\gamma)}{\cos(\gamma-\alpha)} \quad (29)$$

$$N_{rafter,Rd} = f_{c,\alpha,d} \cdot \frac{A_{c,ef,tb} \cdot sin(90+\alpha-\gamma)}{sin(90-\beta+\gamma)} \quad (30)$$

$$A_{c,ef,tb} = b.t_{S,ef,tb} + (b - 2b_S).t_{TM,ef,tb} \quad (31)$$

$$t_{TM,ef,tb} = \frac{t_{TM}-t_S}{cos(\alpha)} \quad (32)$$

$$N_{rafter,Rd} = f_{c,\alpha,d} \cdot A_{c,ef,tb} \quad (33)$$

where:

$N_{rafter,Rd}$ is the design rafter load-bearing capacity;

$f_{c,\alpha,d}$ is the design compressive strength inclined under an angle α to the grain at the tie beam side;

$f_{c,\beta-\alpha,d}$ is the design compressive strength inclined under an angle $\beta - \alpha$ to the grain at

	the rafter side;
α	is the inclination angle of the front-notch surface with respect to the normal of the grain in the tie beam;
β	is the rafter skew angle;
γ	is the inclination angle of the bottom-notch surface with respect to the grain in the tie beam;
$A_{ef,rafter}$	is the effective compressive stressed area at the front-notch surface in the rafter;
$A_{ef,tb}$	is the effective compressive stressed area at the front-notch surface in the tie beam;
b	is the tie beam width;
b_S	is the shoulder width in the tie beam;
t_S	is the shoulder heel depth in the tie beam;
$t_{S,ef,rafter}$	is the effective compressive length in the shoulder at the rafter side;
$t_{S,ef,tb}$	is the effective compressive length in the shoulder at the tie beam side;
t_{TM}	is the TM heel depth in the tie beam;
$t_{TM,ef,rafter}$	is the effective compressive length in the Tenon-Mortise at the rafter side;
$t_{TM,ef,tb}$	is the effective compressive length in the Tenon-Mortise at the tie beam side.

4. Discussion about design models

Although new design models have been defined by gathering all the geometrical and design recommendations available from European Standards and literature referenced to, their reliability and the emergence conditions of both failure modes (i.e. the shear crack and the crushing) have still to be discussed for the three Step Joints (SJ) typologies overviewed in the present paper. So far, several specimens of Single Step Joint (SSJ) have been tested under monotonic compression in the rafter by modifying the SSJ geometrical parameters from the work of Verbist et al. [24]. Thereby, the reliability of SSJ design equations and the emergence conditions of both failure modes have been discussed and checked. Relating to the shear crack in the tie beam, it has been shown that the reducer coefficient $k_{v,red}$*=0.8* accounting for the non-uniform shear stresses over the shear length must be applied for the ratio between the shear length and heel depth $l_v/t_v \geq 6$ whereas $k_{v,red}$=1 can be suggested for the other SSJ geometrical configurations. Furthermore, the inclination angle α of the front-

notch surface has a significant impact on the emergence conditions of shear crack and on the shear capacity of the joint [24]. As future contributions to the research of de Rijk and Jorissen [23] on the non-uniform shear stress distribution along the grain in the tie beam, empirical relationships about the reducer coefficient $k_{v,red} = f(\alpha\,, l_v/t_v)$ should be determined through Finite Element Models in order to improve much more the reliability of SSJ design equations against the shear crack.

The SSJ design equations against the crushing at the front-notch surface are reliable for the GCID whereas they become too restrictive for the GCPTB and GCPR with the rafter skew angle $\beta \geq 30°$ [24], when estimating the design compressive strength $f_{c,\alpha,d}$ through the Norris's Criterion (5)-(6)-(7). For moderated inclination angles of compressive loading to the grain ($\alpha \geq 30°$), higher values of $f_{c,\alpha,d}$ can be obtained with the modified Norris's Criterion (8) [6, 23], which can then be used instead of (5)-(6)-(7) in order to enhance the reliability of proposed SSJ design equations against the crushing. . Besides, they could also be restrictive because the friction inside the connection has been neglected, as research assumption. Thereby, the friction forces at the contact surfaces within the Single Step Joint should ideally be taken into account in the design equations for moderate rafter skew angles ($\beta \geq 30°$).

This discussion and the related design recommendations stated above could also be applied when designing the Double Step Joint and Single Step Joint with Tenon-Mortise in respect with the shear crack and the crushing. Nevertheless, future experimental and numerical assessments on these two SJ typologies are required to check the reliability of design equations and the appearance conditions of both failure modes, by modifying their main geometrical parameters. Furthermore, the design models have been determined by considering no significant eccentricity (d_{supp}) between the joint node and the support area of the timber truss as illustrated in Figure 2. Hence, the previous design equations defined for the three SJ typologies are relevant if the eccentricity d_{supp} is smaller than the tie beam height h_{tb} [9]. Otherwise, the significant eccentricity between the joint node and the

support area will entail additional shear, bending and tension stresses in the cross-section of the tie beam, which requires added design verifications not detailed in the present work.

5. Conclusion

Through the Analytical Campaign, several geometrical configurations of Step Joints (SJ) have been overviewed and sorted out into three typologies: the Single Step Joint (SSJ), the Double Step Joint (DSJ), and the Single Step Joint with Tenon-Mortise (SSJ-TM). By gathering all the geometrical and design recommendations available from the European Standards and authors of works, new design models have been determined for these three SJ typologies in respect with both failure modes: the shear crack in the tie beam, and the crushing at the front-notch surface. So far, the reliability of SSJ design equations have been discussed and checked [24] although some improvement of the design model against the shear crack could be promoted through ongoing numerical assessments on the non-uniform shear stress distribution in the tie beam. Regarding the other two SJ typologies, it is difficult to discuss about the reliability of design models proposed in the present paper without getting any experimental or numerical data as background. Therefore, Experimental Campaigns and Numerical Assessments are going to be performed on several DSJ and SSJ-TM geometrical configurations, by more focusing on the emergence conditions of shear crack as this brittle failure mode may cause the collapse of the whole timber truss. However, it should be clarified that the SJ design models introduced in the present paper are relevant if all the research assumptions previously stated in the research method are met:

- No significant eccentricity between the joint node and the support area of timber trusses;
- Axial force in the rafter only (i.e. no dynamic or out-off-plane loadings);
- Negligible friction forces at the SJ contact surfaces;
- Low and moderate skew rafter angle ($\beta \leq 50°$) [9];

- Checking the geometrical recommendations related to the three SJ typologies [6];
- The connections must be exempt of any damage.

When dealing with any restoration project of existing timber roof structures, Step Joints may be subject to natural damage over time (i.e. shrinkage splitting, insect attacks, fungi decay) because they are constantly in contact with moist masonry supports. Unless introducing some reducer coefficients, the current design models cannot be used to predict the emergence of both failure modes and the maximal load-bearing capacities for damaged Step Joints. Nevertheless, all these equations and recommendations from the present paper can be established as knowledge basis when designing the three SJ typologies in respect with both failure modes, even if these design models may be led to future improvements and adjustments case by case.

Acknowledgements

This work was financed by FEDER funds through the Competitively Factors Operational Programme – COMPETE and by national funds through FCT – Foundation for Science and Technology within the scope of the project PTDC/EPH-PAT/2401/2014 and PhD Scholarships SFRH/BD/128580/2017. This work was partly financed in the framework of the Portuguese Public Procurement Code, LOTE 3ES2 – Escola Secundária de Loulé e Olhão. Parts of this publication are based upon work from COST Action FP1402, supported by COST (European Cooperation in Science and Technology). Furthermore, parts of this paper were firstly published in: *Design of Connections in Timber Structures. A state-of-the-art report by Working Group 3 of COST Action FP1402 – Eds. Carmen Sandhaas, Jørgen Munch-Andersen and Philipp Dietsch – Shaker Verlag Munich, Germany, 2018*.

References

[1] Yeomans D (2003). *The repair of historic timber structures*. Thomas Telford Ltd, London.

[2] Oslet, G. (1890). *Traité de charpente en bois. Encyclopédie théorique & pratique des connaissances civiles et militaires. Partie Civile, Cours de construction, Quatrième partie* – Edited by Chairgrasse H. Fils, Paris, France. Digital reproduction.

http://gallica.bnf.fr/ark:/12148/bpt6k872975z.r=Oslet,+Gustave.langF

[3] NBN EN 1995-1-1 (2004). Eurocode 5 – *Design of timber structures – Part 1.1: General – Common rules and rules for buildings*. CEN, European Standardisation Institute. December 15, 2004, Brussels, Belgium.

[4] DIN 1052:2004-08, (2004). Deutsche Norm - *Design of timber structures—general rules and rules for buildings.* DIN Deutsches Institut für Normung e. V., Praxishandbouch Holzbau. August 2004, Germany.

[5] SIA 265:2012, Swiss Norm SN505:265 (2012) *Bâtiment génie civil - Construction en bois.* Société suisse des ingénieurs et des architectes (SIA). Swiss Standardization Institute. January 2012, Zurich, Switzerland.

[6] Siem, J., Jorissen, A. (2015). Can Traditional Carpentry Joints be assessed and designed using modern standards? *Structural Health Assessment of Timber Structures. Shatis'15: 3rd International Conference on Structural Health Assessment of Timber Structure*, Volume 1 – Edited by Jerzy Jansienko, Tomasz Nowak. Wroclaw – Poland, September 9-11, 2015.

[7] Siem, J. (2017). The single-step Joint – a traditional carpentry joint with new possibilities. *International Wood Products Journal* – Volume 8, Supplement 1, Pages 45-79. DOI:10.1080/20426445.2017.1302148

[8] Bocquet, J-F. (2015). *Les assemblages de charpentes traditionnelles dans le futur contexte réglementaire. Eurocode 5 : Conception et calcul des structures en bois – Sous-partie : Assemblage*. Formation ENSTIB. Université de Lorraine, France.

[9] Allais, M., Kupferle, F., Rossi, F. (2015). *Dimensionnement à froid des assemblages traditionnels bois conformément aux Eurocodes. Guide Pratique*. Supported by CODIFAB and C4CI. December 2015, Paris, France.
http://www.codifab.fr/sites/default/files/guide_pratique_dimensionnement_a_froid_des_assemblasse_traditionnels_dec_2015.pdf

[10] Grezel, J. (1950). Les assemblages. *Annales de l'Institut Techniques du Bâtiment et des Travaux Publics, Manuel de la charpente en bois, n°9* – Institut Technique du Bâtiment et des Travaux Publics – Novembre 1950, Paris, France.

[11] Goss, W.F.M. (1890). *Bench Work in Wood. A course of Study and Practice Designed for the use of schools and colleges*. – Published by Ginn & Company – Boston, USA (1890).
http://www.woodworkslibrary.com/repository/bench_work_in_wood.pdf

[12] Descamps, T. (2015). *Dimensionnement et Technologie des Structures en Bois. Introduction à l'Eurocode 5.* Volume 1 – Matériau, vérification ELU et ELS et assemblages – Université de Mons, Faculté Polytechnique – 4 juin 2015.

[13] Heimeshoff, B., Köhler, N. (1989). *Untersuchung über das Tragverhalten von*

zimmermannsmässigen Holzverbindungen. *Forschungsbericht*. Lehrstuhl für Baukonstruktion und Holzbau Technische Universität München, Germany, December 1989.

[14] Görlacher, R., Kromer, M. (1991). *Tragfähigkeit von Versatzanschlüssen in historischen Holzkonstruktionen*. Bruderverlag, Karlsruhe, Germany. Edited by Bauen Mit Holz. March 1991.

[15] Parisi, M.A., Piazza, M. (2000). Mechanics of plain and retrofitted traditional timber connections. *Journal of Structural Engineering*: ASCE 126(12):1395–1403.

[16] Parisi, M.A., Cordié, C. (2010). Mechanical behaviour of double-step timber joints. *Construction and Building Materials*: Volume 24, Issue 8, August 2010, Pages 1364-1371.

[17] Faye, C., Garcia, P., Magorou, L.L., Rouger, F. (2008). Mechanical behaviour of traditional timber connections: proposals for design, based on experimental and numerical investigations. Part 1: birdsmouth. *CIB – W18. Meeting 41*, August 24-28, 2008, St. Andrews, Canada.

[18] Villar, J.R., Guaita, M., Vidal, P., Arriaga, F. (2006). Analysis of the Stress State at the Cogging Joint in Timber Structures. *Biosystems Engineering*: Volume 96, Issue 1, January 2007, Pages 79-90.

[19] Aira, J.R., Descamps, T., Van Parys, L., Léoskool, L. (2015). Study of stress distribution and stress concentration factor in notched wood pieces with cohesive surfaces. *European Journal of Wood and Wood Products:* Volume 73, Issue 3, May 2015, Pages 325–334.

[20] Munafò, P., Stazi, F., Tassi, C., Davi, F. (2015). Experimentation on historic timber trusses to identify repair techniques compliant with the original structural-constructive conception. *Construction and Building Materials*. Volume 87, July 2015, Pages 54-66.

[21] Feio, A.O., Lourenço, P.B., Machado, J. S. (2014). Testing and modelling of a traditional timber mortise and tenon joint. *Materials and Structures*: Volume 47, Issue 1–2, March 15, 2013, Pages 213–225

[22] Sobra, K., de Rijk, R., Aktas, Y.D., Avez, C., Burawska, I., Branco, J.M. (2016). Experimental and Analytical Assessment of the Capacity of Traditional Single Notch Joints and Impact of Retrofitting by Self-Tapping Screws. *Historical Earthquake-Resistant Timber Framing in the Mediterranean Area.* H. Cruz et al. (Eds.), August 2016, Pages 359-369. DOI10.1007/978-3-319-39492-3_30

[23] de Rijk, R., Jorissen, A. (2016). Spanningen in een Tandverbinding. *Onderzoeksmiddag construeren met hout : 22 januari 2016*. Jorissen, A.J.M., Leijten, A.J.M. (Eds.), Technische Universiteit Eindhoven, Nederland. Pages 42-69. ISBN : 978-90-386-3993-2

[24] Verbist, M., Branco, J.M., Poletti, E., Descamps, T., Lourenço, P.B. (2017). Single step joint: Overview of European standardized approaches and experimentations. *Materials and Structures* – 50: 161 - DOI 10.1617/s11527-017-1028-4 – March 27, 2017.

[25] Verbist, M., Branco, J.M., Poletti, E., Descamps, T., Lourenço, P.B. (2017). Single and Double

Step Joints Design: Overview of European standard approaches compared to experimentation. *Proceedings of the Third International Conference on Preservation, Maintenance and Rehabilitation of Historical Buildings and Structures REHAB 2017* – Green Lines Institute for Sustainable Development, Braga, Portugal, 14-16 June 2017. Pages 1185 – 1194.

[26] Branco J. M., Descamps T. (2015). Analysis and Strengthening of carpentry joints. *Construction and Building Materials.* Volume 97, 30 October 2015, Pages 34-47.

[27] DIN 1052-2 (1988). *Deutsch Norm – Structural use of timber – Mechanicaly fastened joints – Part 2*. DIN Deutsches Institut für Normung e. V., Praxishandbouch Holzbau. April 1998, Germany.

[28] DIN EN 1995-1-1/NA (2010). *German National Annex – Nationally determined parameters – Eurocode 5: Design of timber structures – Part 1-1: General – Common rules and rules for buildings.* DIN Deutsches Institut für Normung e. V., Praxishandbouch Holzbau. December 2010, Germany.

[29] CNR-DT 206 (2007). *Instructions for the Design, Execution and Control of Timber Structures.* National Research Council (CNR). November 28, 2007,. Rome, Italy.

[30] NEN EN 1995-1-1/NB (2011). *Dutch National Annex – Eurocode 5: Design of timber structures - Part 1-1: General - Common rules and rules for buildings*. April 1, 2011, The Netherlands.

[31] NEN 3852 (1973). *Dutch Norm – TGB 1972 – Timber structures – Technical principles for the design and calculation of building structures.* Dutch Standardization Institute. July 1, 1973, Delft, The Netherlands.

[32] NEN 6760 (1991). *Dutch Norm – TGB 1990 – Timber structures – General principles – Requirements and determination methods*. Dutch Standardization Institute. December 1, 1991, Delft, The Netherlands.

[33] NEN 6760 (2005). *Dutch Norm – TGB 1990 – Timber structures – Basic requirements and determination methods*. Dutch Standardization Institute. May 1, 2005, Delft, The Netherlands.

[34] NS 446 (1957): *Norvegian Standard – Rules for the calculation and execution of wooden constructions* – April 25, 1957, Oslo, Norway.

[35] NBN EN 1995-1-1/A1 (2008). *Eurocode 5 – Amendment 1 – Design of timber structures – Part 1.1: General – Common rules and rules for buildings* – CEN, European Standardisation Institute. November 26, 2008, Brussels, Belgium.

[36] Descamps, T. (2013). *Carpentry connections*. *Training school on assessment and reinforcement of timber elements*. COST FP1101, December 9-13, 2013, University of Mons, Belgium.

List of Figures

List of Tables

Figures:

Fig. 1 Step Joint and elements constituting the traditional timber carpentry (King-Post truss).

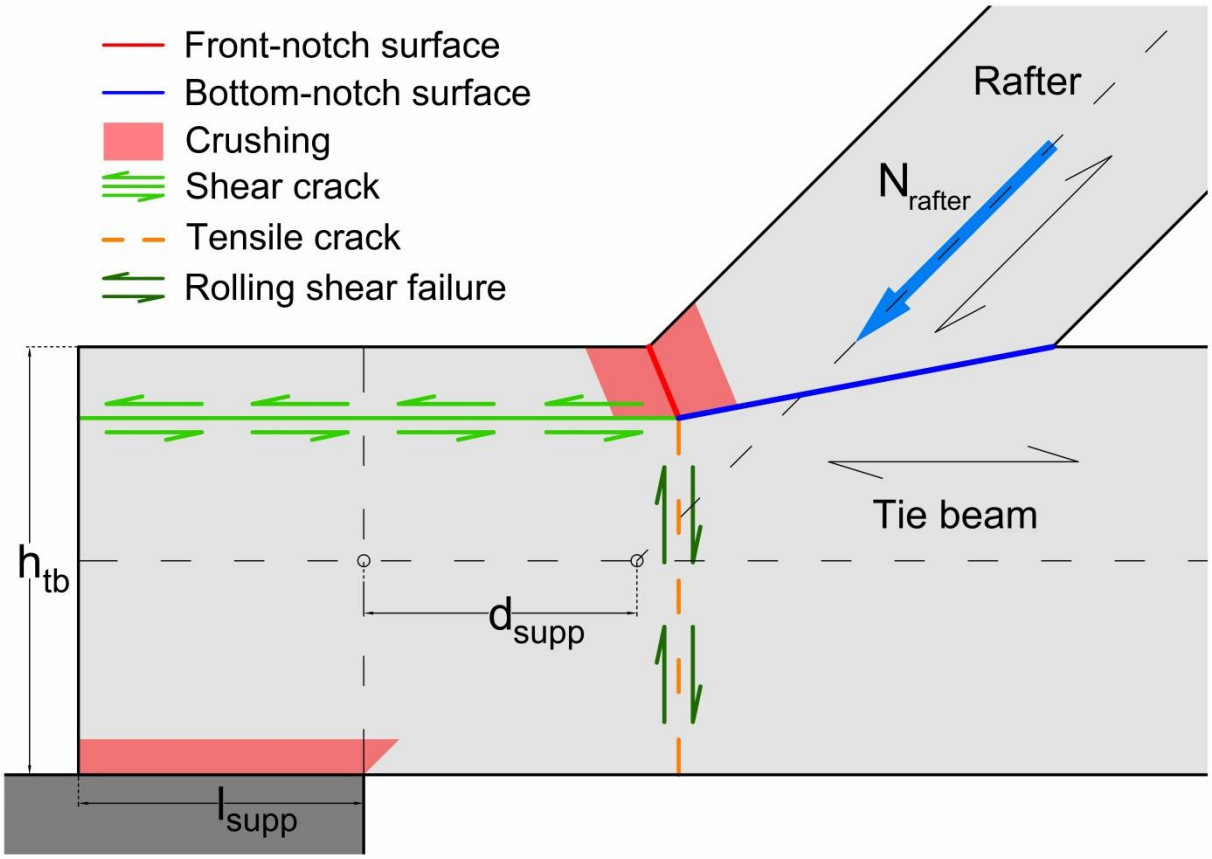

Fig. 2 Illustration of different failures modes likely to occur in the Single Step Joint.

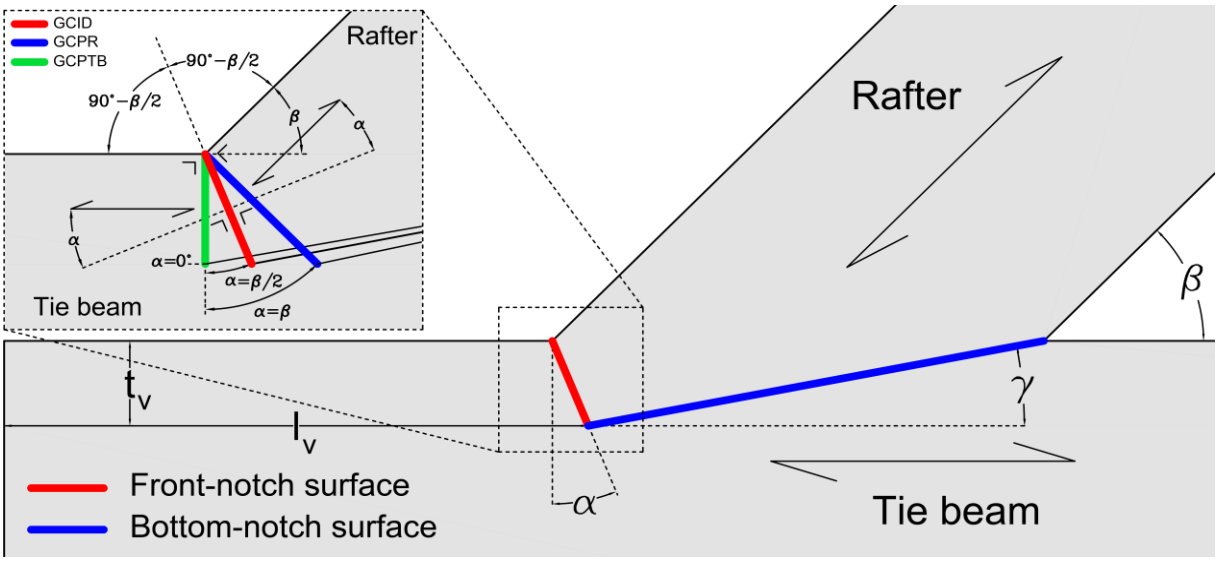

Fig. 3 General SSJ geometrical parameters and different inclination of the front-notch surface according to the three SSJ families [24].

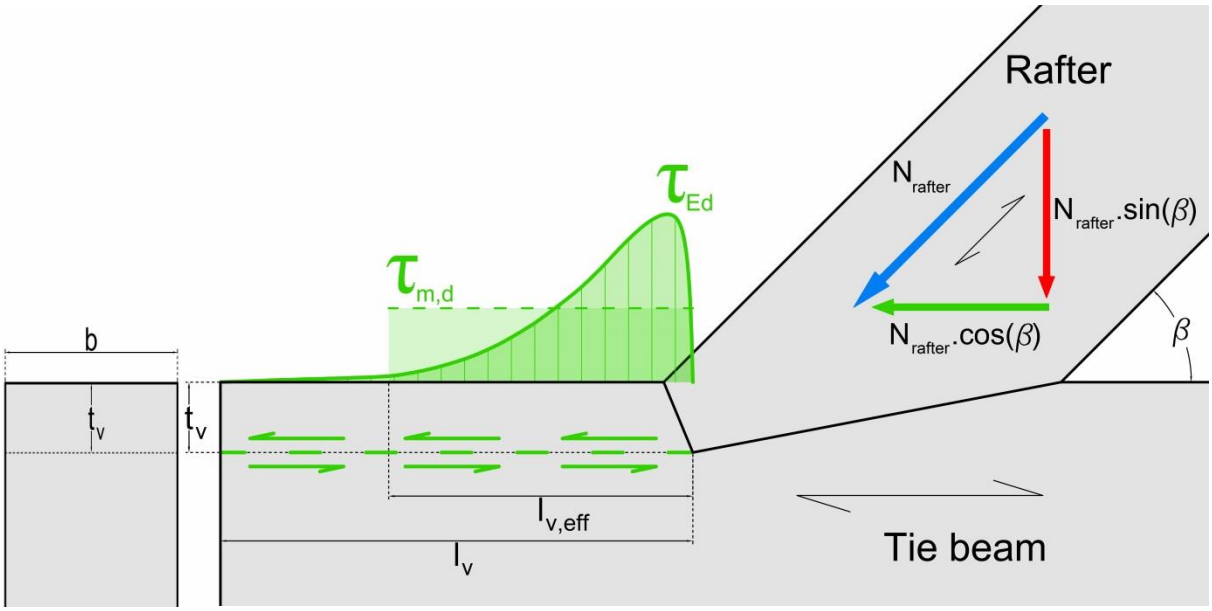

Fig. 4 Illustration of the non-uniform shear stress distribution τ_{Ed}, at the heel depth t_v parallel to the grain in the tie beam, in comparison with the uniform average shear stress $\tau_{m,d}$ assumed in (11) [24].

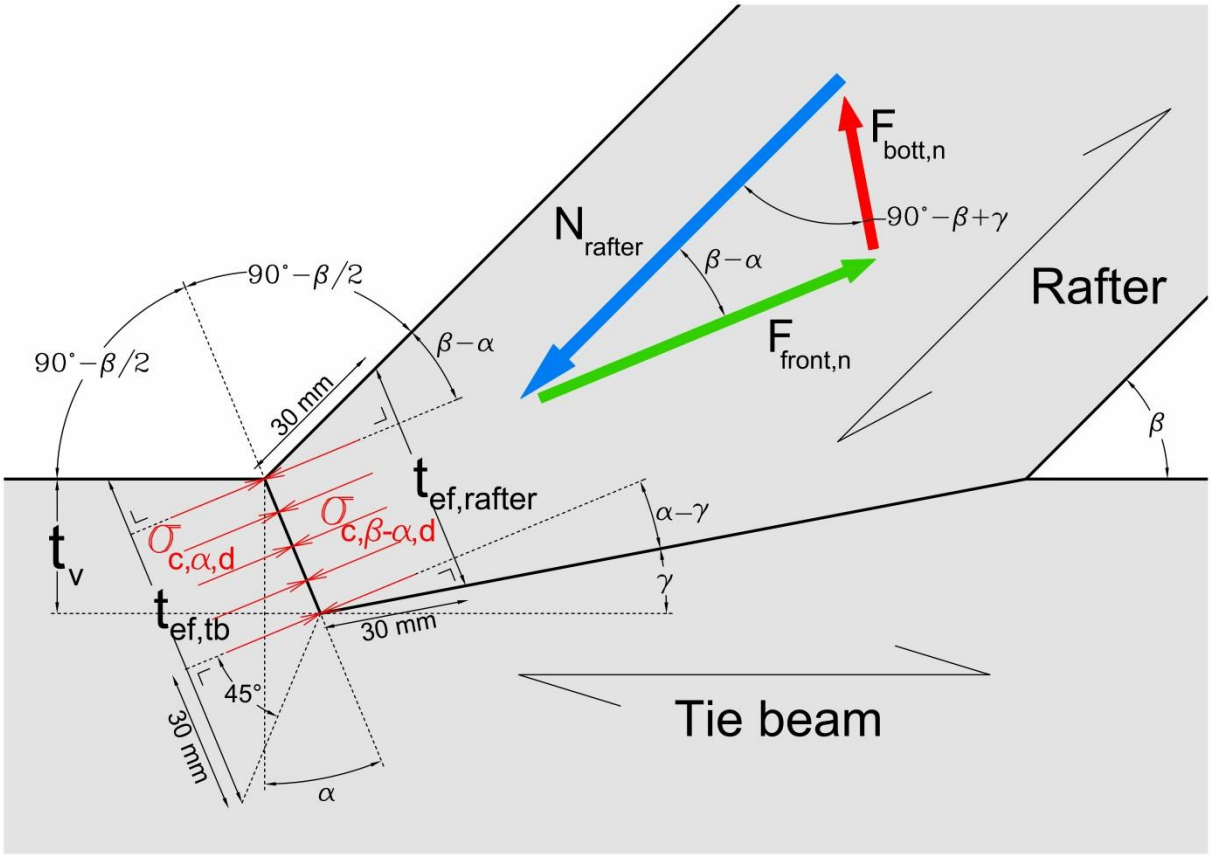

Fig. 5 Schema of the effective lengths $t_{ef,rater}$ and $t_{ef,tb}$, respectively in the rafter and tie beam for SSJ geometrical configurations [24].

Fig. 6 Illustration of Double Step Joint on-site [36].

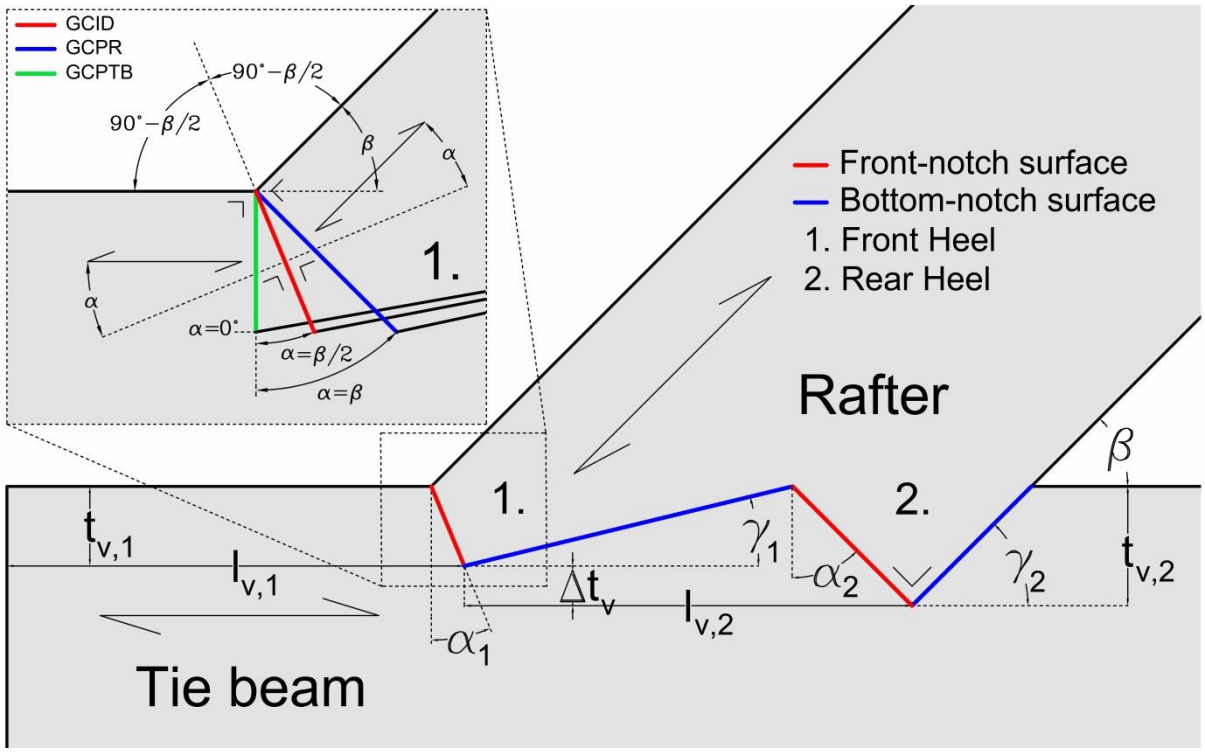

Fig. 7 General DSJ geometrical parameters and inclination of the front-notch surface in the Front heel according to the three SSJ families [25].

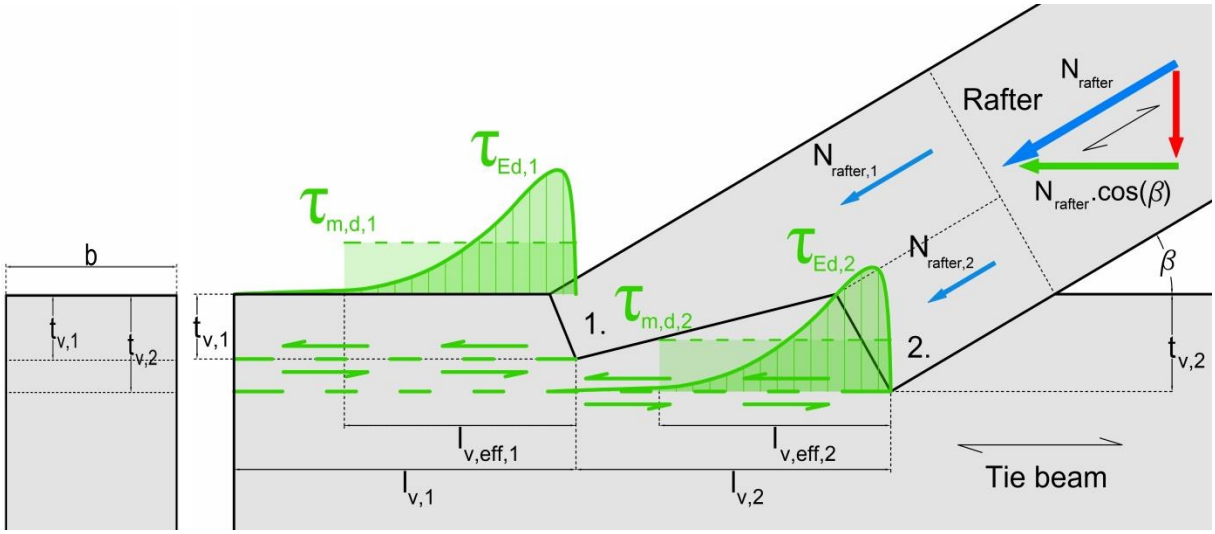

Fig. 8 Illustration of the non-uniform shear stress distributions $\tau_{Ed,i}$ at the Front and Rear Heels depths in the tie beam, in comparison with their uniform average shear stresses $\tau_{m,d,i}$ assumed in (19) [25].

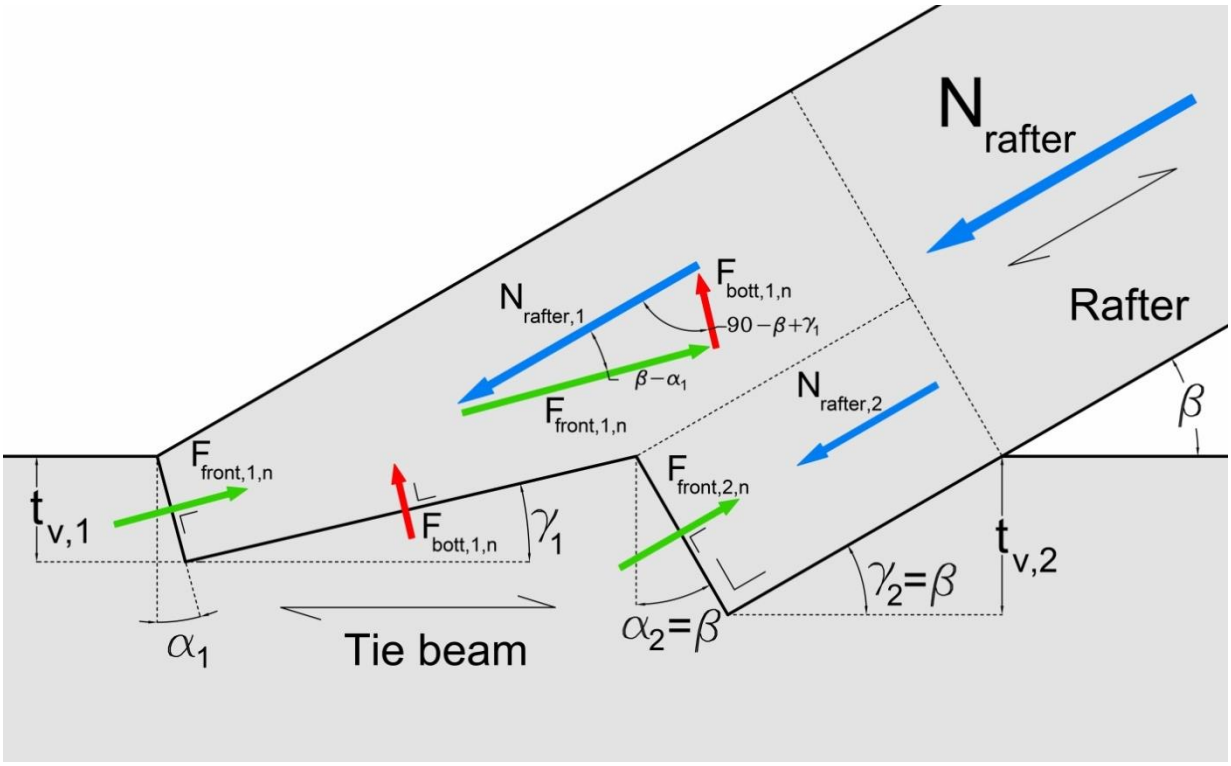

Fig. 9 Schema of the internal forces resolution in the Front and Rear Heels of the Double Step Joint [25].

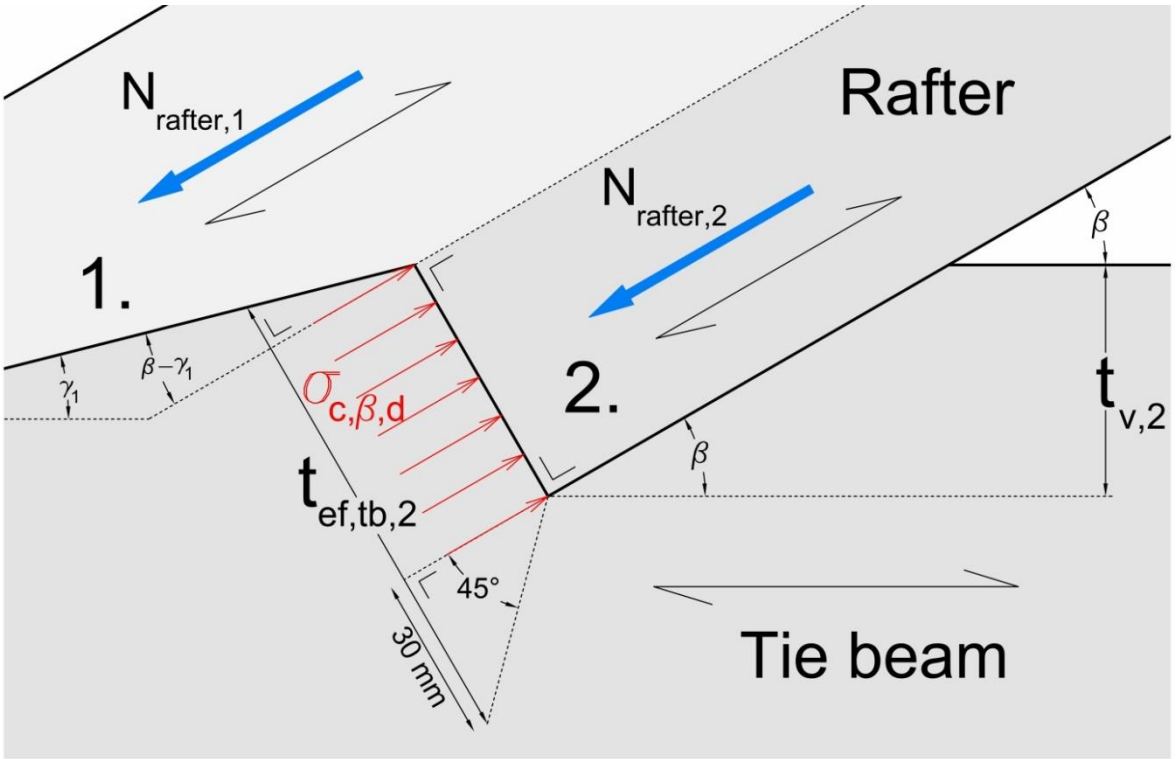

Fig. 10 Schema of the effective length $t_{ef,tb,2}$ in the tie beam at the front-notch surface in the Rear Heel [25].

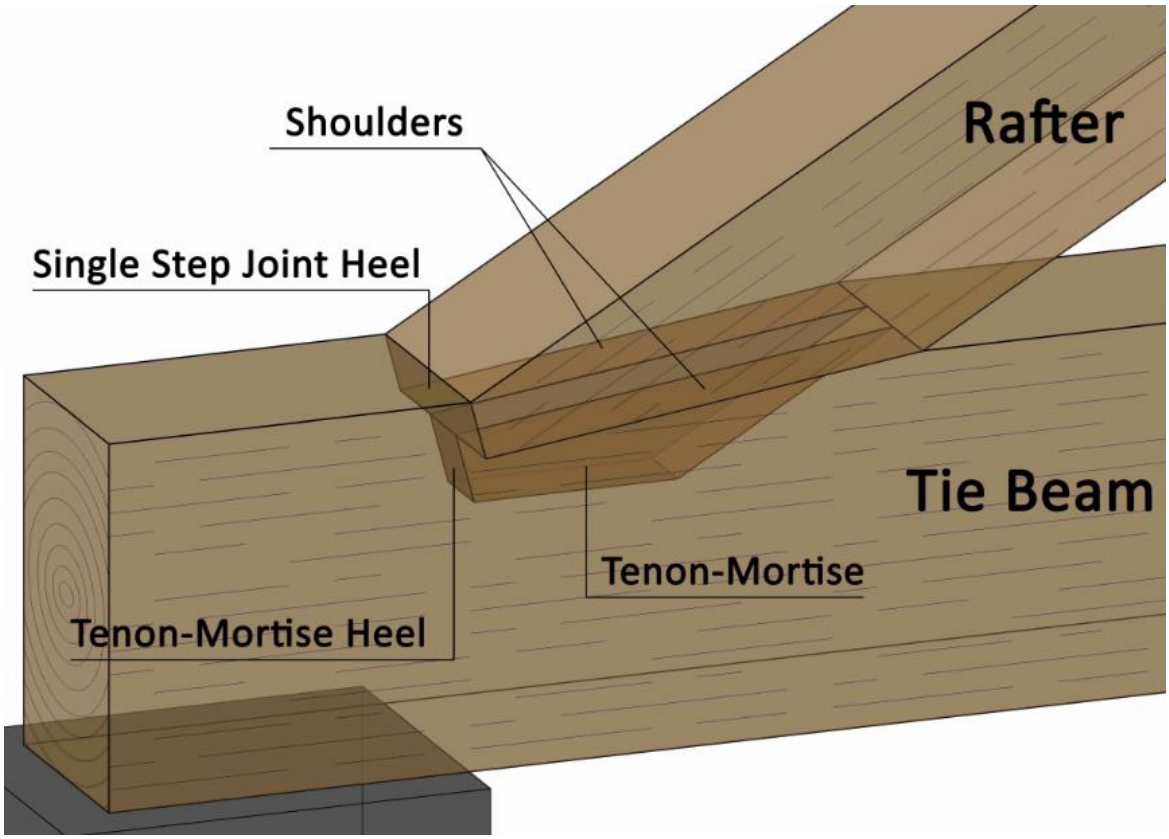

Fig. 11 Components of the Single Step Joint with Tenon-Mortise.

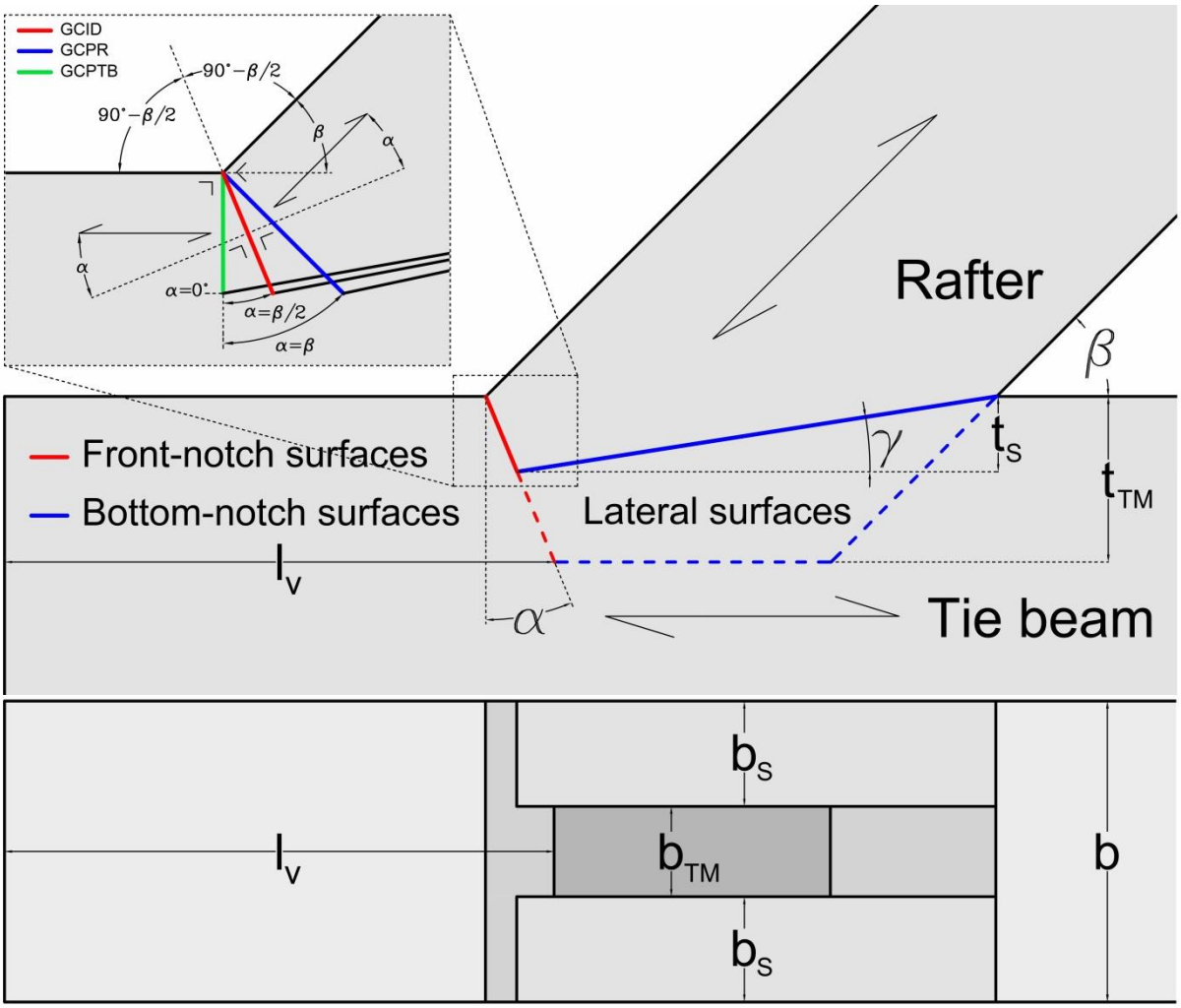

Fig. 12 General SSJ-TM geometrical parameters and inclination of the front-notch surface according to the three SSJ families.

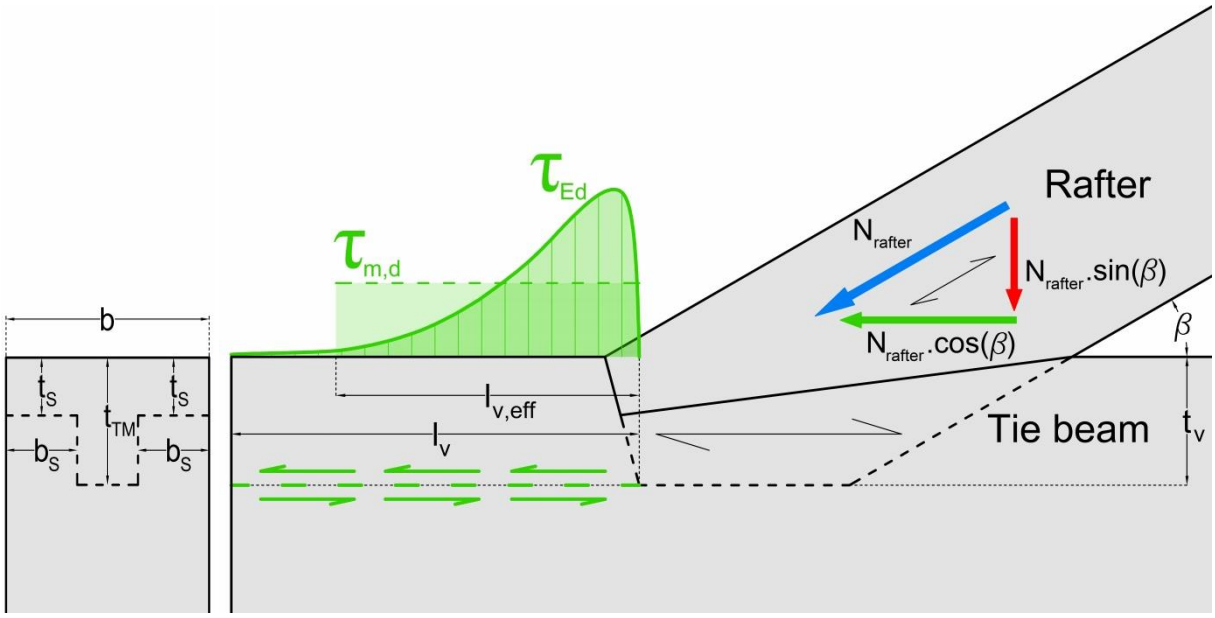

Fig. 13 Illustration of the non-uniform shear stress distribution τ_{Ed}, at the TM heel depth along the grain in the tie beam, in comparison with the uniform average shear stress $\tau_{m,d}$ assumed in (11).

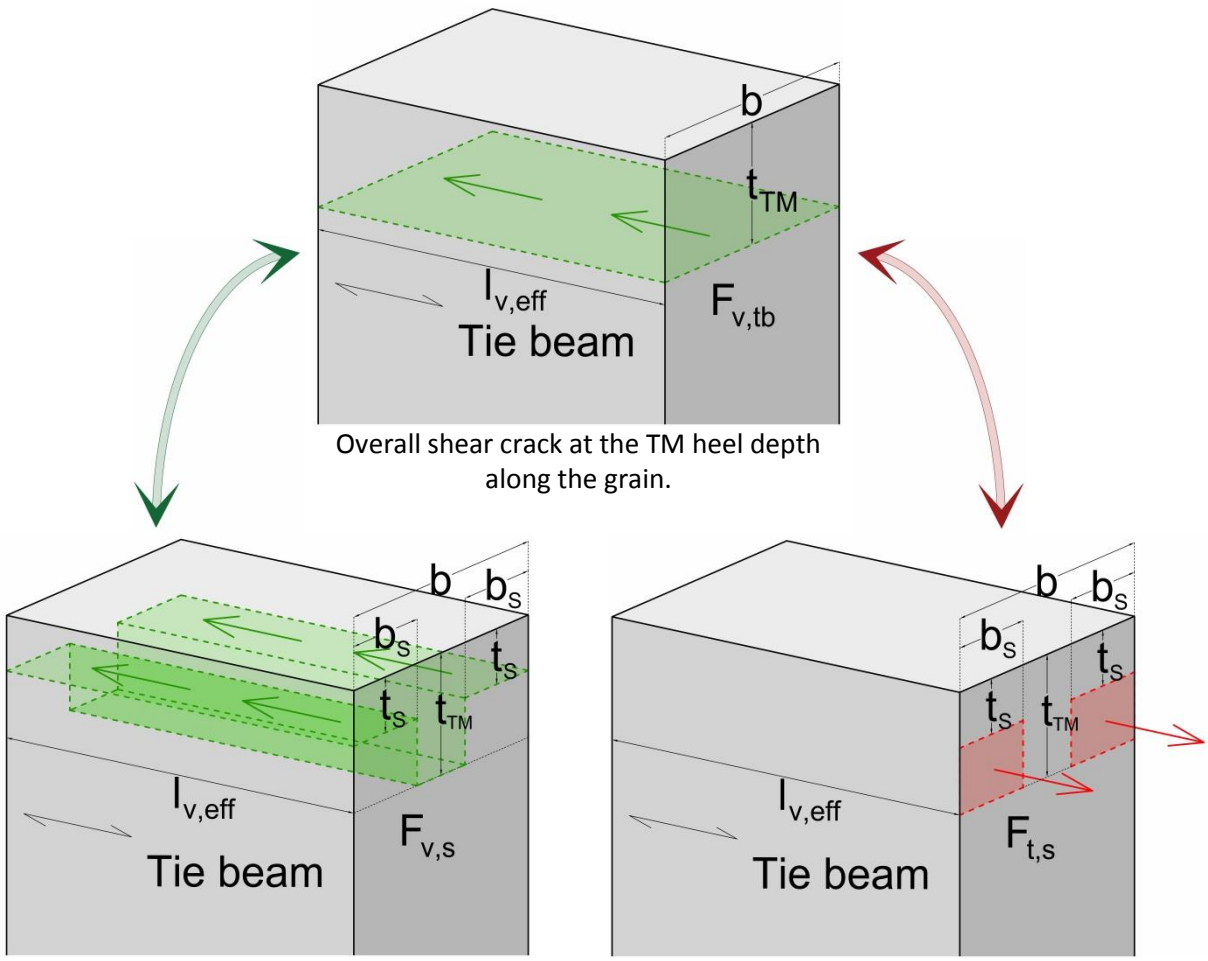

Fig. 14 Overall shear crack and subcategories of failure modes at the TM heel depth along the grain in the tie beam.

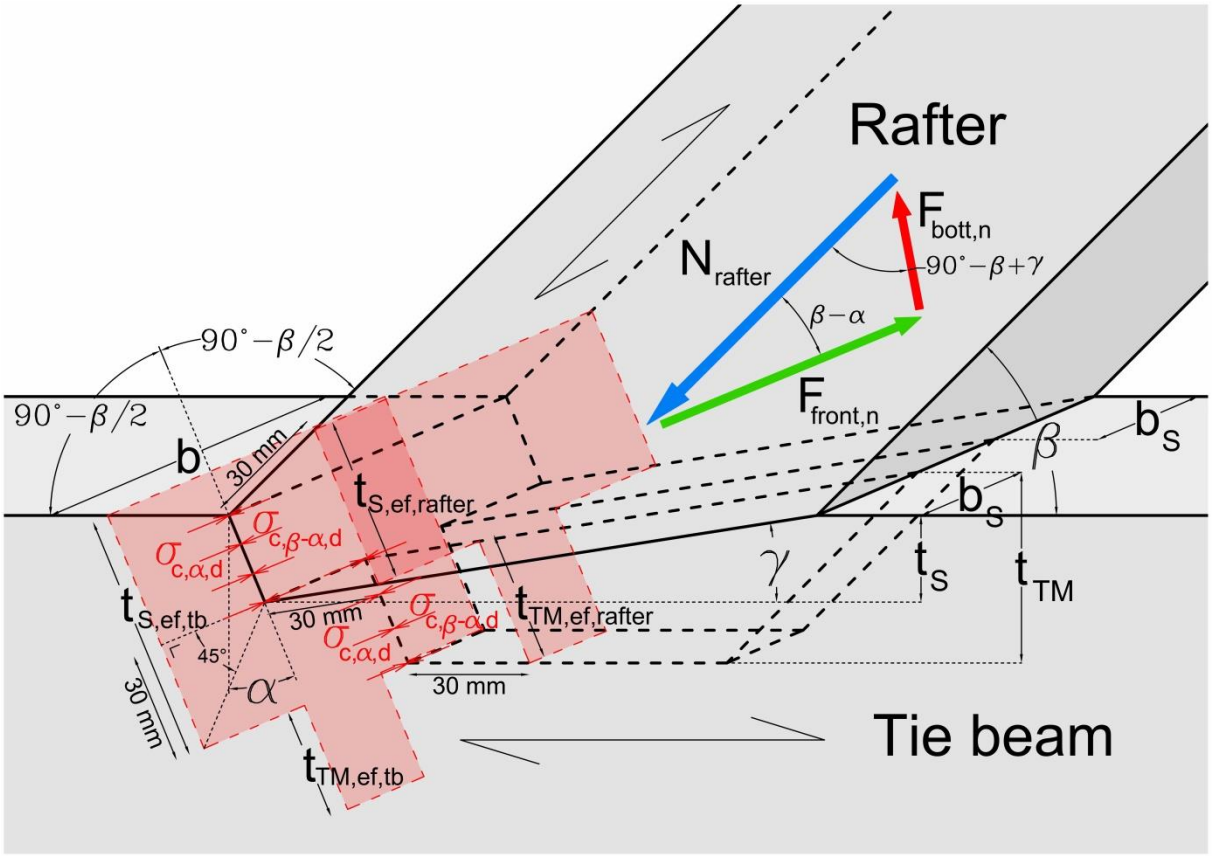

Fig. 15 Schema of the effective lengths $t_{S,ef,rafter}$, $t_{TM,ef,rafter}$, $t_{S,ef,tb}$ and $t_{TM,ef,tb}$, in the shoulder (*S*) and the Tenon-Mortise (*TM*) at the rafter (*rafter*) and tie beam (*tb*) sides, respectively.

Tables:

Table 1 Geometrical recommendations on the SSJ geometrical parameters with respect to the tie beam height h_{tb}, from different national Standards [6].

	Germany [4, 27, 28], Italy [29], Switzerland [5]			The Netherlands [30, 31, 32, 33]		Norway [34]		
β	$\leq 50°$	$50° \leq \beta \leq 60°$	$\geq 60°$	$\leq 50°$	$\geq 50°$	$\leq 50°$	$50° \leq \beta \leq 60°$	$\geq 60°$
t_v	$\leq \frac{h_{tb}}{4}$	Linear Interpolation	$\leq \frac{h_{tb}}{6}$	$\leq \frac{h_{tb}}{4}$	$\leq \frac{h_{tb}}{5}$	$\leq \frac{h_{tb}}{4}$	$\leq \frac{h_{tb}}{5}$	$\leq \frac{h_{tb}}{6}$
l_v	$\geq 150\ mm$ [5]		$\leq 8\ .\ t_v$ [4] $\geq 200\ mm$ [4]	$\geq 6\ .\ t_v$		$\geq 150\ mm$		
α	$\frac{\beta}{2}$ [5]		$\gamma \leq \alpha \leq \beta$ [4]	$\frac{\beta}{2} \leq \alpha \leq \beta$		$\frac{\beta}{2}$		

Table 2 Recommendations about the DSJ geometrical parameters, derived from national Standards [6].

	Netherlands [30]	Germany [4], Switzerland [5]	Italy [29]	Norway [34]
β	$\leq 50°$	----------	----------	$\leq 45°$
$t_{v,1}$	----------	$\leq \frac{h_{tb}}{6}$	$\leq 0{,}8\ .\ t_{v,2}$	$\leq \frac{h_{tb}}{4}$
$t_{v,2}$	----------	$\leq \frac{h_{tb}}{4}$	----------	$\geq \frac{h_{tb}}{4}$
Δt_v	$\geq 15\ mm$	$\geq 10\ mm$	$\geq 10\ mm$	$15\ mm \leq \Delta t_v \leq 20\ mm$
$l_{v,1}$	$\geq 6\ .\ t_{v,1}$	$\leq 8\ .\ t_{v,1}$ [4] $\geq 200\ mm$ [4] $\geq 150\ mm$ [5]	----------	----------
$l_{v,2}$	----------	$\leq 8\ .\ t_{v,2}$ [4]	----------	----------